2019 IEEE Intl Conf on Parallel & Distributed Processing with Applications, Big Data & Cloud Computing, Sustainable Computing & Communications, Social Computing & Networking (ISPA/BDCloud/SocialCom/SustainCom)

Underwater Image Enhancement with a Total Generalized Variation Illumination Prior

Zhengjie Zhao†, Yuxiang Dai†, Peixian Zhuang*
School of Electronic and Information Engineering
Nanjing University of Information Science and Technology, Nanjing 210044, China
*Corresponding email: **zhuangpeixian0624@163.com**

***Abstract*—In order to promote the visual quality of degraded underwater images, we develop an innovative variational model based on Retinex with a total generalized variation (TGV) prior on the illumination. The TGV prior is adopted to approximate piecewise smoothness and piecewise linear smoothness of the illumination, which combines the first-order and second-order total variation (TV) to model the variation of illumination. When adopting this illumination prior in the Retinex-based algorithm, the illumination and reflection are well separated, and underwater enhanced results appear more natural and their details and edges are better preserved. Then an efficient iterative optimization method is derived to settle the proposed model via alternately calculating the illumination and the reflection simultaneously. Numerous experiments on both visual results and objective metrics demonstrate the superiority of our method compared with several underwater enhancement methods. In addition, the proposed method can be extended for dehazing, sandstorm removal and low illumination image enhancement, which can illustrate better capacity of our model.**

Keywords- Underwater image enhancement; Total generalized variation; Retinex; Alternating optimization.

I. INTRODUCTION

Owing to the growing extraction of marine resources, high-quality underwater images are of great significance for human exploration and excavation. Concerning the underwater image, there are two interfering factors [1]: one is that light is absorbed and scattered in the water due to suspended particles before reaching the camera, which leads to low contrast and atomization. Another is that the wavelength influences the attenuation of light, and the salinity of water and dissolved organic compounds promote different levels of color deviation. Therefore, underwater images are likely to be bluish or greenish, and they appear underexposed and blurry. Plentiful algorithms are created to settle above problems, and existing methods are classified into three categories:

Model-free Methods Model-free methods adjust the pixel values of an image to advance the visual quality without explicitly modeling the image formation process. For the color correction methods, Chambah et al. [2] proposed an unsupervised color equalization algorithm on the basis of the ACE model, whose results are robust and have local filtering properties. Based on a low-level image feature-based color constancy hypothesis, Henke et al. [3] employed a distance map to remove the color casts of underwater images by estimating multiple factors, but image details or structures are not preserved well. For the integration methods, Ancuti et al. [4] designed a fusion-based underwater image and video enhancement method, which can suppress noise and avoid under-exposure. Fu et al. [5] presented a variational framework for Retinex with an effective alternating direction optimization strategy, which can yield better brightness and sharpness in enhanced underwater images. However, these methods may over-enhance images, and their results may lose some details.

Model-based Methods Model-based methods are established from the degradation process of underwater images, through estimating model parameters and inverting degradation process, better underwater images are obtained. Trucco et al. [6] designed a self-adjusting underwater image restoration filter based on the simplified Jaffe-McGlamery underwater imaging mathematical model, which can reduce the illumination scattering effect of an image to some extent. Galdran et al. [7] put forward a Red Channel method for degraded underwater images, and colors related with short wavelengths can be restored. Li et al. [8] proposed a restoration strategy based on blue-green channels dehazing with red channel correction to solve color deviation and contrast loss of underwater images. However, these methods are limited to assumptions and priors, which can lead to unreal underwater images.

Deep Learning-based Methods Different from the above-mentioned methods, deep learning-based approaches learn the direct mapping between clear scenes and degraded images. Li et al. [9] developed WaterGAN with an end-to-end network, including a module to estimate the depth and a color correction module. Fabbri et al. [10] improved the quality of underwater images via Generative Adversarial Networks (GANs), which can improve input to vision-driven behaviors. The enhanced underwater images appear more natural in details, however, these methods take a long time to train deep learning models.

In this paper, we design a variational model based on Retinex with a total generalized variation [11] illumination prior to enhance single underwater image. Our model exhibits

†The co-first authors contributed equally. This work was supported in part by the National Natural Science Foundation of China under Grant 61701245, in part by The Startup Foundation for Introducing Talent of NUIST 2243141701030, in part by College Students Practice Innovation Training Program of NUIST 201910300079Y, in part by A Project Funded by the Priority Academic Program Development of Jiangsu Higher Education Institutions.

978-1-7281-4328-6/19/$31.00 ©2019 IEEE
DOI 10.1109/ISPA-BDCloud-SustainCom-SocialCom48970.2019.00147

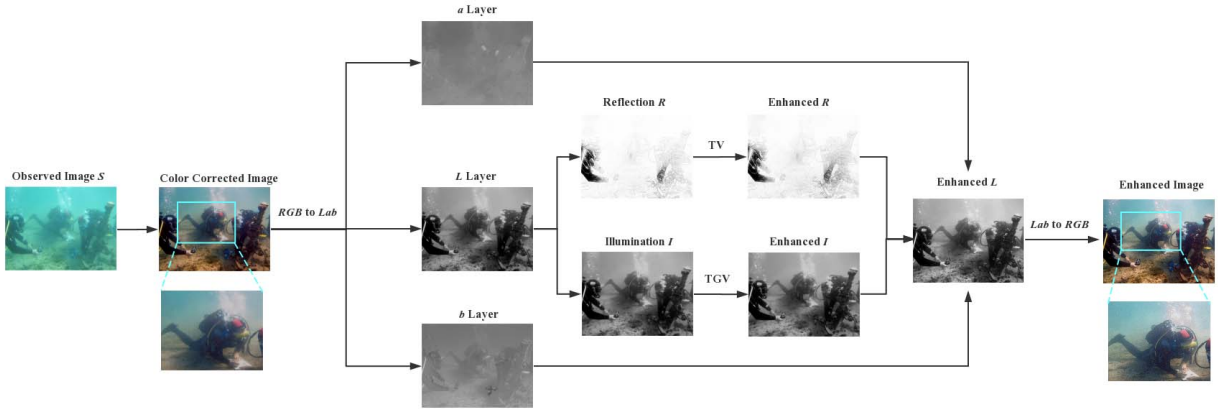

Figure 1: The flowchart of the proposed method.

three appealing contributions as follows:

- We propose a Retinex-based variational model to promote the visual quality of underwater images by introducing a total generalized variation (TGV) prior on the illumination. The TGV prior is adopted to model the illumination variation in the Retinex algorithm, and it combines first-order and second-order total variation to approximate the piecewise smoothness and piecewise linear smoothness of the illumination. We establish an effective model in which the illumination varies smoothly and moderately, and underwater enhanced results appear more natural and preserve more structures than other competitive methods.
- We develop an efficient iterative optimization strategy to settle the proposed model via an alternating calculation between the illumination and the reflection.
- We provide numerous experiments to reveal the superiority of our method in terms of visualization results and objective metrics. Additionally, the proposed method can be extended for dehazing, sandstorm removal and low illumination images enhancement, which demonstrates the applicability of the proposed method.

II. PROPOSED METHOD

Fig. 1 is the flow chart of our method, where the quality of input underwater image has been promoted by our method. The proposed method is divided into three main steps: color correction, Retinex-based decomposition with a total generalized variation (TGV) prior, and post-processing. Firstly, we employed a simple and effective color correction method [5] in a degraded underwater image for removing color casts and preserving image naturalness. Then the proposed Retinex-based model with a TGV illumination prior is used to estimate the illumination and the reflection simultaneously. After that, a post-processing on the histogram is utilized [5], [18] to avoid blurs and under-exposure. The steps of color correction, Retinex-based decomposition with a TGV prior, and post-processing will be detailed in the following subsections.

A. Color Correction

When light is traveling underwater, most of the underwater images are bluish or greenish due to light attenuation at various wavelengths [12]. A statistical-based color correction strategy [5] is exploited for color casts removal, and the color corrected image is calculated below:

$$\begin{aligned} S^{\sigma}_{CR} &= \frac{(S^{\sigma} - S^{\sigma}_{min})}{(S^{\sigma}_{max} - S^{\sigma}_{min})} \times 255 \\ S^{\sigma}_{max} &= S^{\sigma}_{mean} + \theta S^{\sigma}_{var} \\ S^{\sigma}_{min} &= S^{\sigma}_{mean} - \theta S^{\sigma}_{var} \end{aligned} \tag{1}$$

where $\sigma \in \{R, G, B\}$, S denotes an observed underwater image, and S^{σ}_{CR} is the color corrected image. S^{σ}_{mean} and S^{σ}_{var} are mean square error (MSE) and mean value in σ channel. S^{σ}_{max} and S^{σ}_{min} are the maximum and minimum of the channel separately. θ is a positive parameter that controls the dynamic of images.

B. Model Construction

Considering the consistency between the change of underwater environment and the variation of illumination, the Retinex algorithm can be applied to decompose the reflection (R) and the illumination (I) from L layer of S_{CR}. The formula is $L = R \cdot I$ [13]-[16], where $\cdot$ denotes the element-wise multiplication. Underwater image enhancement methods using Retinex are effective in terms of sharpening, color fidelity, dynamic range compression and color constancy. However, previous Retinex-based methods may lead to halo artifacts around edges and universal grey in low contrast areas, and most importantly, their models for the illumination are not accurate and effective, which only focus on the big scales in images' first-order gradient field, but the nature of the illumination usually follows certain paths since it varies relatively slower.

To settle the mentioned problems, we established a variational model on the basis of Retinex to enhance underwater images by introducing a total generalized variation (TGV) [12] prior on the illumination:

$$\begin{aligned} \underset{(R,I)}{argmin} \|I \cdot R - L\|_2^2 + \alpha\|DI - p\|_1 \\ +\beta\|DR\|_1 + \gamma\|\varepsilon(p)\|_1 \quad s.t. \quad L \leq I \end{aligned} \tag{2}$$

where positive parameters α,β,γ are used to balance the above terms, D is the difference operator in directions of horizontal and vertical. R is ranged from 0 to 1, therefore the constraint is $I \geq L$. The term $\|I \cdot R - L\|_2^2$ denotes the data fidelity to constrain consistency between $I \cdot R$ and L, the term $\|DR\|_1$ refers to TV reflectance sparsity, which can enforce piece-wise continuous of reflectance. The rest terms are the TGV prior which are employed to approximate piecewise smoothness and piecewise linear smoothness of the illumination, and first-order and second-order total variations are combined to accurately and effectively model underwater images larger-scale edges and fine-scale details. Owing to adapting TGV to illumination, $p = (p_1, p_2)$ is the symmetrized gradient of the deformation field, $\varepsilon(p)$ is the symmetrized derivative and is defined as:

$$\varepsilon(p) = \begin{bmatrix} \partial_x p_1 & \frac{(\partial_y p_1 + \partial_x p_2)}{2} \\ \frac{(\partial_y p_1 + \partial_x p_2)}{2} & \partial_x p_2 \end{bmatrix} \tag{3}$$

C. Optimization Algorithm

Traditional gradient descent or other discrete optimization methods cannot be used to deal with two unknown variables in the proposed model (2). Therefore, a high-efficiency iterative optimization scheme is derived to settle our model by iteratively calculating R and I alternately. An auxiliary variable d is firstly employed to approximate the TV reflection term, and the model (2) is adapted below:

$$\begin{aligned} \underset{(R,I,d)}{argmin} \|I \cdot R - L\|_2^2 + \alpha\|DI - p\|_1 + \beta\|d\|_1 \\ +\lambda\|DR - d\|_1 + \gamma\|\varepsilon(p)\|_1 \quad s.t. \quad L \leq I \end{aligned} \tag{4}$$

Before taking our proposed optimization strategy, we use the Gaussian low-pass filtering to avoid the severe oscillation of illumination intensity, the initialization of I is defined to be the Gaussian low-pass filtered image L. And we set the initialization $R = 0$.

Update for Reflection. d is updated with shrinkage operator [5] under the given R:

$$\begin{aligned} d_x &= shrink(D_x R, \frac{1}{2\lambda}) \\ d_y &= shrink(D_y R, \frac{1}{2\lambda}) \end{aligned} \tag{5}$$

where $shrink(x, \varepsilon) = \frac{x}{|x|} * max(|x| - \varepsilon, 0)$, and x and y are directions of horizontal and vertical.

Preset d and I, update R by

$$R = F^{-1}\frac{F(\frac{L}{I}) + \beta\lambda F(D^T d)}{F(1) + \beta\lambda(F^*(D_x) \cdot F(D_x) + F^*(D_y) \cdot F(D_y))} \tag{6}$$

where F and F^* are the Fast Fourierc Transform (FFT) operator and its complex conjugate respectively. FFT avoids very-large-matrix inversion by diagonalizing derivative operators, which can accelerate the calculation process. And all calculations are performed in the component-wise operation.

Update for Illumination. Then four auxiliary variables $(k, l; m, n)$ and two positive penalty parameters (φ_1,φ_2) [11], [17] are introduced to transform the formula (2) as follows:

$$\begin{aligned} \underset{(R,I,k,l,m,n)}{argmin} \|I \cdot R - L\|_2^2 + \lambda_1\|k\|_1 + \frac{\varphi_1}{2}\|k - DI + p - m\|_2^2 \\ +\lambda_2\|l\|_1 + \frac{\varphi_2}{2}\|l - \varepsilon(p) - n\|_2^2 \quad s.t. \quad L \leq I \end{aligned} \tag{7}$$

To calculate the value of I, we set variables $(p, k, l; m, n) = 0$, $(\lambda_1, \lambda_2, \varphi_1, \varphi_2) > 0$ in the initialization to obtain the following Euler equation:

$$I - \varphi_1 div(\nabla I) = f - \varphi_1 div(k + p - m) \tag{8}$$

The above equation can be addressed by

$$I_{i,j} = \Re(F^{-1}(\frac{F(\frac{L}{R} - \varphi_1 div(k + p - m))}{1 - 2\varphi_1(\cos\frac{2\pi s}{W} + \cos\frac{2\pi r}{H} - 2)})) \tag{9}$$

where (i, j) is the position of image pixel, div denotes the divergence operator, and $\Re$ is a complex number's real part. When computing p and fixing variables $(I, k, l; m, n)$, we can derive the Euler equation related with $p = (p_1, p_2)$. For each p_1 and p_2, we have the following discrete formulations:

$$\begin{aligned} (\varphi_1 - \varphi_2\partial_x^+\partial_x^- - \frac{\varphi_2}{2}\partial_y^+\partial_y^-)p_{1i,j} - \frac{\varphi_2}{2}\partial_y^+\partial_x^- p_{2i,j} = q_{1i,j} \\ (\varphi_1 - \frac{\varphi_2}{2}\partial_x^+\partial_x^- - \varphi_2\partial_y^+\partial_y^-)p_{2i,j} - \frac{\varphi_2}{2}\partial_y^+\partial_x^- p_{1i,j} = q_{2i,j} \end{aligned} \tag{10}$$

and their solutions are calculated:

$$\begin{aligned} p_{1i,j} &= \Re(F^{-1}(\frac{c_{22}F(q_{1i,j}) - c_{12}F(q_{2i,j})}{G})) \\ p_{2i,j} &= \Re(F^{-1}(\frac{c_{11}F(q_{2i,j}) - c_{21}F(q_{1i,j})}{G})) \end{aligned} \tag{11}$$

When computing k and l and fixing variables $(I, p, l; m, n)$, we have the equation for 2D vector k:

$$\lambda_1\frac{k}{|k|} + \varphi_1(k - \nabla I + p - m) = 0 \tag{12}$$

and its solution is:

$$\begin{aligned} k_{i,j} = \max(|\nabla I_{i,j} - p_{i,j} + m_{i,j}| - \frac{\lambda_1}{\varphi_1}, 0) \\ \times \frac{\nabla I_{i,j} - p_{i,j} + m_{i,j}}{|\nabla I_{i,j} - p_{i,j} + m_{i,j}|}\frac{L}{R} \end{aligned} \tag{13}$$

After that, the Euler equation with respect to l is given

$$\lambda_2\frac{l}{|l|} + \varphi_2(l - \varepsilon(p) - n) = 0 \tag{14}$$

and its solution is derived:

$$l_{i,j} = \max(|\varepsilon(p_{i,j}) + n_{i,j}| - \frac{\lambda_2}{\varphi_2}, 0)\frac{\varepsilon(p_{i,j}) + n_{i,j}}{|\varepsilon(p_{i,j}) + n_{i,j}|} \tag{15}$$

We update the iterative parameter m of Bregman from m to $m + \nabla I - p - k$, and update the iterative parameter n

of Bregman from n to $n + \varepsilon(p) - l$. Then we repeat the procedures above until I becomes convergent. Finally, the proposed algorithm is summed up in **Algorithm 1**, and the detail of TGV illumination calculation ($TGV(\cdot)$) is presented in **Algorithm 2**.

Algorithm 1 Summary of Our Algorithm

Input: observed image L, parameters p, α, β, γ
Initialization: $I^0 \leftarrow$ Gaussian filtering of L, and $R^0 = 0$.
At the i-th iteration:
Update d^i via Eq. (5).
Update R^i via Eq. (6).
Update $I^i \leftarrow TGV(L/R^i)$.
Stop iteration when total energy no longer decreases.
Output: enhanced results R' and I'.

Algorithm 2 TGV Illumination Calculation

1: Initialization: $(p, k, l; m, n) = 0, (\lambda_i, \varphi_i) > 0, i = 1, 2.$
2: Update I via Eq. (9).
3: Update p via Eq. (11).
4: Update k via Eq. (13).
5: Update l via Eq. (15).
6: Update m from m to $m + \nabla I - p - k$.
7: Update n from n to $n + \varepsilon(p) - l$.
8: Repeat above steps until I is convergent.

D. Post-processing

When R and I are calculated, a histogram-based post-processing [5], [18] is exploited to settle the problems of blurring and underexposure. And we employed contrast-limited adaptive histogram equalization (CLAHE) [14] to acquire the enhanced reflection (R_e). In the meantime, the histogram specification of the illumination ($I' = \arctan(I)$) is adjusted to make exposure bright enough, which not only avoids underexposure but also preserves the light naturalness. In line with the cumulative density function's (CDF) definition, the formula is:

$$H(z) = \frac{\Sigma_{i=0}^{z} I'(i) \cdot h(i)}{\Sigma_{i=0}^{\max(z)} I'(i) \cdot h(i)} \tag{16}$$

where z and max(z) are the z-th and maximum gray level of I respectively, h represents the amount of z-th gray levels. To light up dark areas and prevent over-enhancement, the specified histogram region is constrained:

$$C(f(t)) = \frac{\Sigma_{j=0}^{t} s(j)}{\Sigma_{j=0}^{230} s(j)} \tag{17}$$

where $s(t) = \arctan(t - 15), t \in [0, 230]$. We can draw that $I_e = C(f^{-1}(H(I)))$, and the processed R and I are combined to achieve the enhanced L layer: $L_e = R_e \cdot I_e$. The final enhanced underwater image is achieved by transforming the *Lab* color space into *RGB*.

III. EXPERIMENTAL RESULTS

Plenty of experiments are conducted to illustrate the effectiveness of our method in underwater image enhancement, and we compare the proposed method with the following seven methods: three model-based methods: Ancuti et al.[4], Fu et al.[5], Fu et al.[19]; three model-free methods: Li et al.[8], Galdran et al.[7], He et al.[20]; one deep learning-based method: Fabbri et al.[10]. The implementation codes of seven competitive approaches are from the authors′ homepage. We evaluate the enhanced images from two points: visual effect and objective evaluation. The objective evaluation metrics UIQM [22] and UCIQE [21] are employed. Higher values of UIQM and UCIQE indicate better underwater image quality. The higher value of UIQM means the better quality of the enhanced image which is the closer to human visual perception, while the higher value of UCIQE indicates the lower degradation of the image which is closer to the original object. In the proposed method, the parameters α, β, γ are respectively fixed as 0.01, 6.5, 7.5, the iteration number of TGV is set to 70, and 5 iterations of alternating direction optimizations are generally performed.

In Fig. 2, Ancuti et al.[4], Fu et al.[19], Li et al.[8], Galdran et al.[7] and He et al.[20] present unpleasant blurrings at the edges of the objects (such as fishes, coral and reefs) in enhanced underwater images, and cannot remove color casts. Although Fu et al.[5] and Fabbri et al.[10] achieve good results of color correction, their enhanced images lose some details and appear over-enhanced in some certain places. However, the visual effect of our results is better in textures, and the color correction results of each objects turn out to be pleasant. And the proposed method preserves more details and looks more natural and mild in certain areas. In the second column of Fig. 2, enhanced images using the proposed method present more naturalness in both contrast and shadow of the images. In the third column of Fig. 2, the brightness variation of the proposed method from the top left to the bottom right shows more natural and coordinated. In the fourth column of Fig. 2, exposure of reefs in our results is appropriate which can avoid over-exposure and preserve better details. In the fifth and seventh columns of Fig. 2, it is noticeable that the proposed method obtains relatively outstanding results in the transition between dark areas and light areas, meanwhile, the details and edges in the image are preserved well. In addition, the quantitative measurements of different underwater enhancement methods using the above two quality assessments are performed on 48 test underwater images which are collected from previous literature, and their corresponding results are detailed in Table 1 where the best results are marked in bold. Compared with other competitive approaches, it is obvious that our method not only generates higher means of UIQM and UCIQE, but also performs well in respective variances which can achieve more stable performance than other methods in different underwater scenes.

To confirm appropriate parameters, we adjust one parameter and fix others during one experiment to investigate the sensitivity of the proposed algorithm in parameter settings. We obtain more appropriate parameters by observing the variation of the UIQM value. Fig. 3 (a) illustrates that the UIQM value fluctuates with the change of iterations using TGV. The UIQM tends to be steady when the number comes to 60 or more, and we stably set the iteration number to 70. Fig. 3 (b) shows

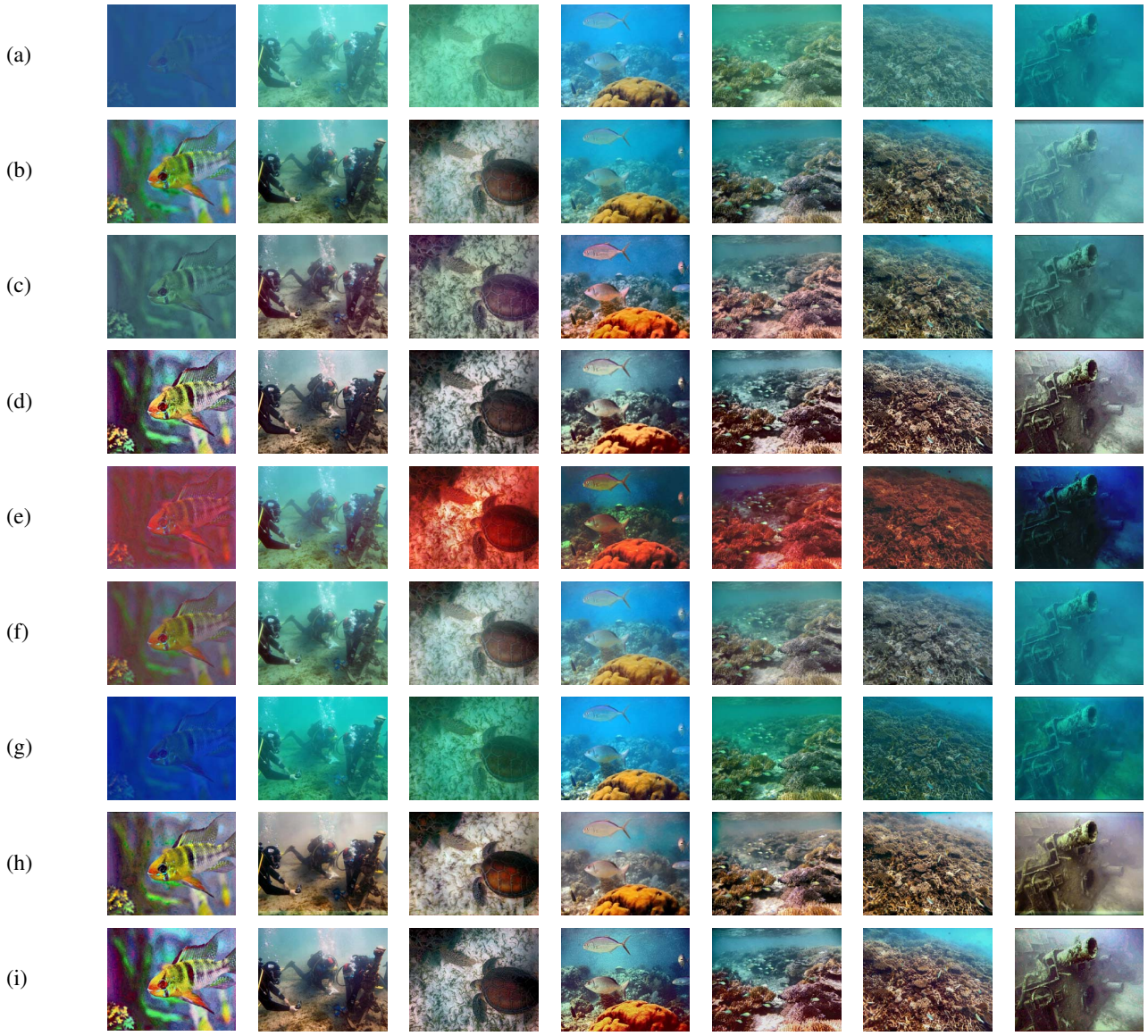

Figure 2: The enhanced results using the proposed method and other seven methods. (a) Raw images. (b) Ancuti et al. [4]. (c) Fu et al. [19]. (d) Fu et al. [5]. (e) Li et al. [8]. (f) Galdran et al. [7]. (g) He et al. [20]. (h) Fabbri et al. [10]. (i) Ours.

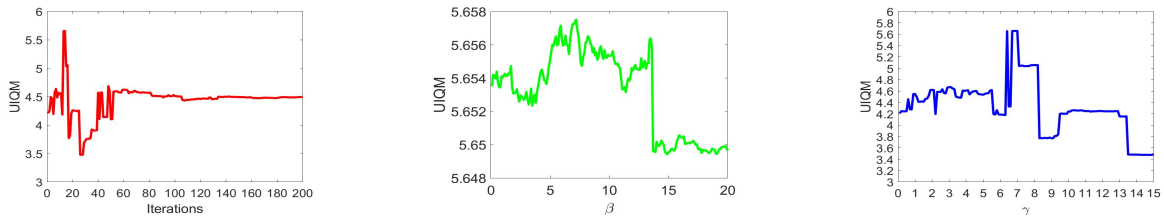

(a) (b) (c)

Figure 3: Parameter evaluation. (a) UIQM vs iterations. (b) UIQM vs weighting parameter β. (c) UIQM vs weighting parameter γ.

TABLE I: Average Mean/Variance of UIQM and UCIQE on 48 underwater images.

	Ours	[4]	[19]	[5]	[8]	[7]	[20]	[10]
UIQM	**4.5018**/ 0.5648	2.8569/ 1.6188	3.3779/ 1.4146	4.4522/ 0.4308	4.2308/ 3.5026	2.7864/ 2.0963	1.0275/ 2.3793	4.1392/ 0.4119
UCIQE	**0.6298**/ 0.0012	0.5622/ 0.0028	0.5350/ 0.0039	0.6274/ 0.0011	0.5512/ 0.0036	0.5467/ 0.0021	0.4819/ 0.0051	0.6093/ 0.0008

TABLE II: The run time (seconds) of five methods on different image sizes.

Method	275×183	550×412	1037×778	1600×1200
Ours	1.81	5.75	16.51	36.61
[4]	0.99	1.00	2.48	4.90
[19]	0.09	0.26	0.86	1.87
[5]	3.01	6.57	49.05	57.11
[7]	0.67	0.98	1.09	1.74

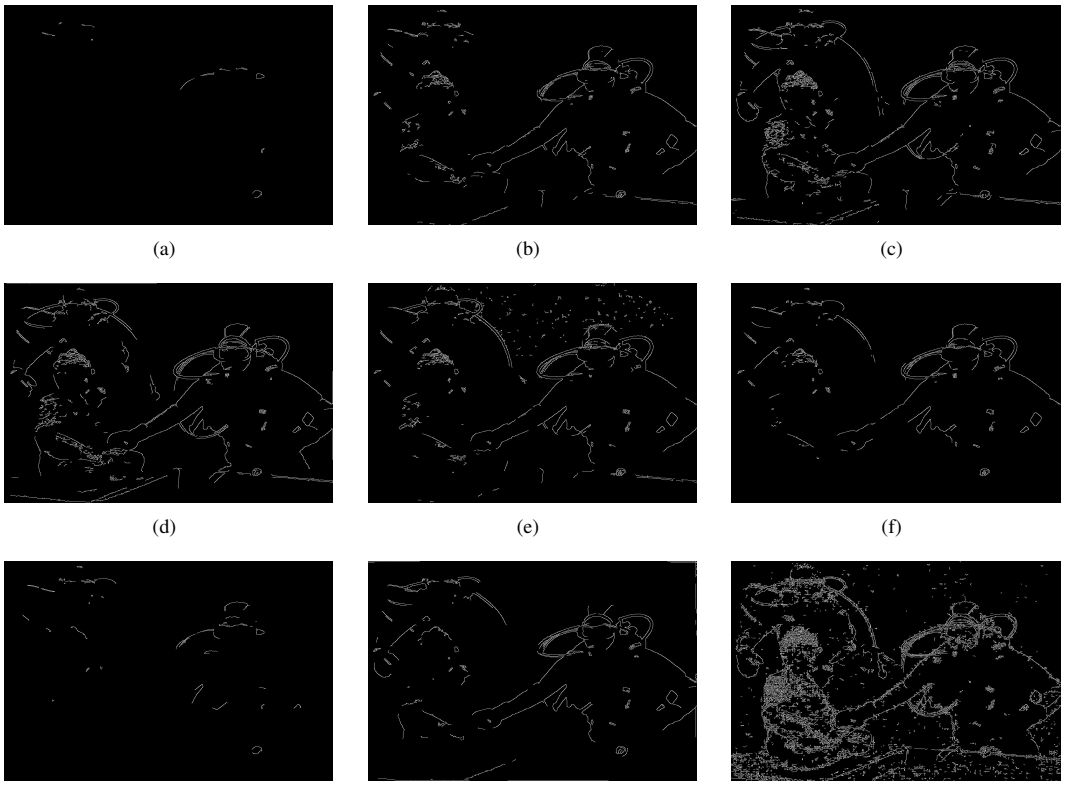

Figure 4: Canny edge detection. (a) Raw image. (b) Ancuti et al. [4]. (c) Fu et al. [19]. (d) Fu et al. [5]. (e) Li et al. [8]. (f) Galdran et al. [7]. (g) He et al. [20]. (h) Fabbri et al. [10]. (i) Ours.

that the UIQM value tends to be stable when the value of β is between 5 and 10, and thus we set β to 6.5, which is nearly the top of the curve. Fig. 3 (c) demonstrates that the UIQM value is high when the value of γ is from 6 to 8, and we eclectically set γ to 7.5. Therefore, these curves of UIQM versus (vs) these parameters in Fig. 3 reveals the rationality of parameter settings discussed above. The runtime experiments of different methods are performed in Table 2. Our method takes more time on the TGV iterations, but we will improve the execution speed of our non-optimized code by adopting more optimizations or parallel computation in the near future.

Furthermore, we extend the proposed method and other rivalrous methods in Canny edge detection [23], [24] to test the quality of detail extraction in Fig. 4, where the proposed method can preserve more abundant details and structures of objects, which outperforms other competitive compared methods. Moreover, we apply the proposed method in dehazing, sandstorm removal and low illumination image enhancement in Figs. 5-7. Although there exists some over-exposure and blurs in the enhanced images, our overall visual results are satisfactory, which demonstrates an extensive application prospect of the proposed method.

(a) (b) (c) (d)

(e) (f) (g) (h)

Figure 5: The dehazing results using the proposed method. (a)-(d) Raw images, (e)-(h) Our dehazed images.

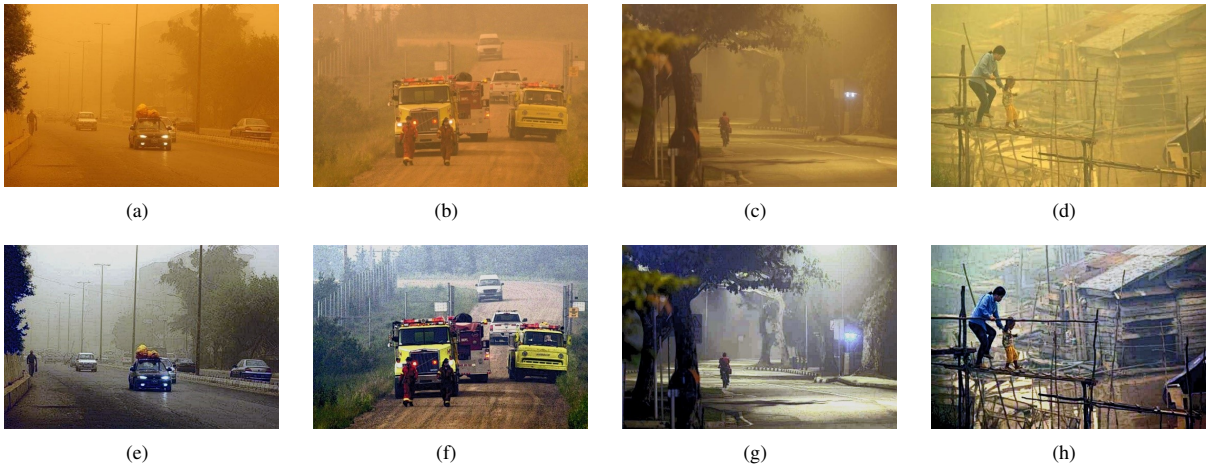

(a) (b) (c) (d)

(e) (f) (g) (h)

Figure 6: The enhanced results of sandstorm images using the proposed method. (a)-(d) Raw images, (e)-(h) Our enhanced images.

IV. CONCLUSION

For enhancing single underwater image, we proposed a Retinex-based variational model which imposes a Total Generalized Variation (TGV) prior on the illumination. Multi-order total variation is employed to model piecewise smoothness and piecewise linear smoothness of the illumination, which can make the illumination smoother and preserve better structures. And a high-efficiency iterative optimization approach is designed for calculating our model by using an alternative calculation of the reflection and the illumination respectively. Experimental results reveal the advantages of the proposed method in visualization and objective evaluations. In addition, we illustrate the capacity of the proposed model for image dehazing and enhancing sandstorm and low illumination images.

REFERENCES

[1] R. Liu, M. Hou, X. Fan, and Z. Luo, "Real-world underwater enhancement: challenging, benchmark and efficient solutions," arXiv preprint arXiv:1901.05320.

[2] M. Chambah, D. Semani, A. Renouf, P. Courtellemont, A. Rizzi, "Underwater color constancy: enhancement of automatic live fish recognition," Color Imaging IX: Processing, Hardcopy, and Applications. International Society for Optics and Photonics, 2003, 5293: 157-168.

[3] B. Henke, M. Vahl, Z. Zhou, "Removing color cast of underwater images through non-constant color constancy hypothesis," IEEE International Symposium on Image and Signal Processing and Analysis, 2013: 20-24.

[4] C. Ancuti, C. O. Ancuti, T. Haber, P. Bekaert, "Enhancing underwater images and videos by fusion," IEEE Conference on Computer Vision and Pattern Recognition, 2012: 81-88.

[5] X. Fu, P. Zhuang, Y. Huang, Y. Liao, X. P. Zhuang, X. Ding, "A retinex-based enhancing approach for single underwater image," IEEE International Conference on Image Processing, 2014: 4572-4576.

[6] E. Trucco, A. T. Olmos-Antillon, "Self-tuning underwater image restoration," IEEE Journal of Oceanic Engineering, 2006, 31(2): 511-519.

[7] A. Galdran, D. Pardo, A. Picn, A. Alvarez-Gila, "Automatic red-channel underwater image restoration," Journal of Visual Communication and Image Representation, 2015, 26: 132-145.

[8] C. Li, J. Quo, Y. Pang, S. Chen, J. Wang, "Single underwater image restoration by blue-green channels dehazing and red channel correc-

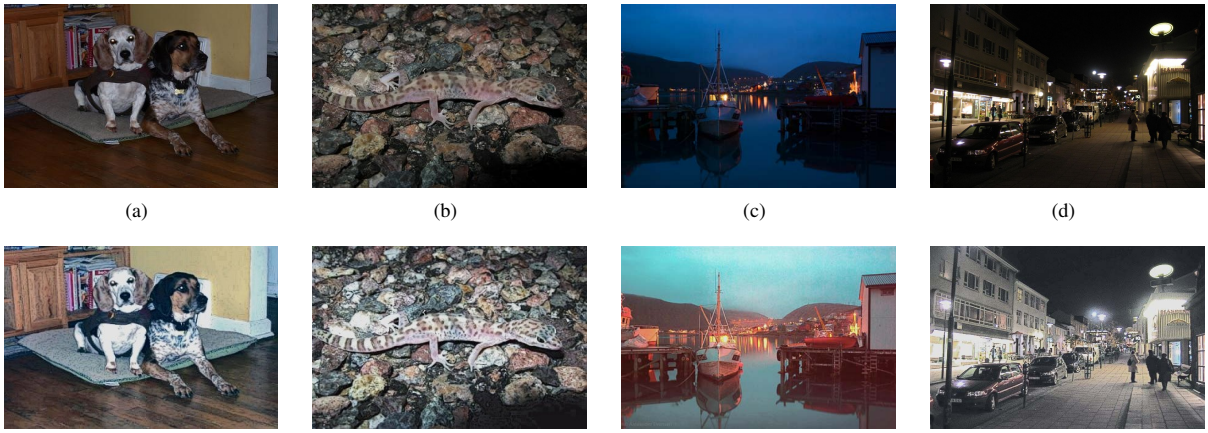

(a) (b) (c) (d)

(e) (f) (g) (h)

Figure 7: The enhanced results of low illumination images using the proposed method. (a)-(d) Raw images, (e)-(h) Our enhanced images.

tion," IEEE International Conference on Acoustics, Speech and Signal Processing, 2016: 1731-1735.

[9] J. Li, K. A. Skinner, R. M. Eustice, M. Johnson-Roberson, "WaterGAN: Unsupervised generative network to enable real-time color correction of monocular underwater images," IEEE Robotics and Automation letters, 2017, 3(1): 387-394.

[10] C. Fabbri, M. J. Islam, J. Sattar, "Enhancing underwater imagery using generative adversarial networks," IEEE International Conference on Robotics and Automation, 2018: 492-526.

[11] K. Bredies, K. Kunisch, T. Pock, "Total generalized variation," SIAM Journal on Imaging Sciences, 2010, 3(3): 492-526.

[12] H. Lu, Y. Li, S. Serikawa, "Underwater image enhancement using guided trigonometric bilateral filter and fast automatic color correction," IEEE International Conference on Image Processing, 2013: 3412-3416.

[13] E. H. Land, "The Retinex. American Scientist," 1964, 52(2): 247-264.

[14] C. Tomasi, R. Manduchi, "Bilateral filtering for gray and color images," IEEE International Conference on Computer Vision, 1998, 98(1): 2.

[15] E. H. Land, J. J. McCann, "Lightness and retinex theory," Journal of the Optical Society of America, 1971, 61(1): 1-11.

[16] G. Wyszecki, W. S. Stiles, "Color science," New York: Wiley, 1982.

[17] W. Lu, J. Duan, Z. Qiu, R. W. Liu, L. Bai, "Implementation of high-order variational models made easy for image processing," Mathematical Methods in the Applied Sciences, 2016, 39(14): 4208-4233.

[18] K. Zuiderveld, "Contrast limited adaptive histogram equalization," Graphics gems IV, 1994: 474-485.

[19] X. Fu, Z. Fan, M. Ling, Y. Huang, X.Ding, "Two-step approach for single underwater image enhancement," International Symposium on Intelligent Signal Processing and Communication Systems, 2017: 789-794.

[20] K. He, J. Sun, X. Tang, "Single image haze removal using dark channel prior," IEEE Transactions on Pattern Analysis and Machine Intelligence, 2010, 33(12): 2341-2353.

[21] M. Yang, A. Sowmya, "An underwater color image quality evaluation metric," IEEE Transactions on Image Processing, 2015 24(12): 6062-6071.

[22] K. Panetta, C. Gao, S. Agaian, "Human-visual-system-inspired underwater image quality measures," IEEE Journal of Oceanic Engineering, 2015, 41(3): 541-551.

[23] Y. Guo, H. Li, P. Zhuang, "Underwater image enhancement using a multiscale dense generative adversarial network," IEEE Journal of Oceanic Engineering, 2019.

[24] J. Canny, "A computational approach to edge detection," Readings in computer vision. Morgan Kaufmann, 1987: 184-203.